ELECTROCHEMICAL STUDIES OF THE CORROSION PERFORMANCE OF CARBON STEEL IN SIMULATED BASALT REPOSITORY ENVIRONMENTS

J. A. Beavers and N. G. Thompson
BATTELLE
Columbus Laboratories
505 King Avenue
Columbus, Ohio 43201

ABSTRACT

The potentiodynamic polarization technique was utilized to evaluate the influence of metallurgical and environmental variables on pitting and SCC susceptibility of carbon steel in simulated basalt repository environments. It was found that carbon steel exhibits active-passive behavior in the nominal basalt groundwater composition and thus these localized failure modes are possible. The metallurgical structure (wrought versus cast), impurity level of the steel and minor variations in steel composition did not have a pronounced effect on the electrochemical behavior. Similarly, a 10-fold concentration of the basalt groundwater composition did not have a pronounced effect on the electrochemical behavior. On the other hand, the individual concentration of several species that may be present in a basalt repository environment did have a significant effect on the electrochemical behavior and there was evidence that synergistic action between these species occurs. In follow-on studies, the single and combined effects of these species on the electrochemical behavior will be quantified.

BACKGROUND

The Nuclear Regulatory Commission (NRC) has proposed Rule 10CFR60 [1] which specifies criteria for disposal of high level radioactive waste in geologic repositories. The proposed criteria include requirements for containment of the waste for a period of 300 to 1000 years and for release of radionuclides at rates of less than 10^{-5} parts per year thereafter.

Two approaches have been considered by the Department of Energy (DOE) for the fabrication of a waste package that will provide containment: a corrosion-resistant package or a corrosion-allowance package. In the former, the package is constructed of a thin (less than 1.5 cm) overpack of a highly corrosion-resistant material such as Titanium Grade 12 or HASTELLOY® Alloy C-276. These alloys rely on thin passive films for their corrosion resistance; under some circumstances, these films can be breached, resulting in localized forms of degradation, such as pitting, crevice corrosion, stress-corrosion cracking (SCC), or hydrogen embrittlement (HE). (HE may also occur in the absence of passive film breakdown, but is less likely where these films are intact.) Since rates of these forms of degradation are quite high in terms of the required life, the licensee of a waste package which utilizes these corrosion-resistant materials is confronted with the difficult task of proving that these localized forms of degradation will not occur under expected operating conditions for a waste repository.

® HASTELLOY is a registered trademark of the Cabot Corporation.

An alternative approach for waste-package construction is to utilize a thick, corrosion-allowance material, such as wrought or cast carbon steel, for the overpack. It is presumed that, with a corrosion-allowance material, general corrosion rates can be accurately predicted and that catastrophic localized forms of corrosion can be avoided. A major problem with this approach is that carbon and low-alloy steels also are susceptible to these localized forms of corrosion under some environmental conditions. Indeed, years of experience with buried steel structures such as natural gas pipelines indicate that localized corrosion is the most likely failure mode for steel components in underground environments.

Accordingly, the study of localized failure modes is a major emphasis of the NRC program on the performance of waste package materials being carried out at Battelle's Columbus Laboratories. Work over the last several years has focused on the pitting and stress-corrosion cracking behavior of carbon steel in a basalt repository environment. Early on in this effort, a survey of the literature was performed to identify stress-corrosion cracking agents for carbon and low alloy steels. [2] A number of species were identified, several of which may be present in a basalt repository environment. These include: carbonates, hydroxides, phosphates, nitrates, chlorides, and oxygen. Phosphates and nitrates may enter a repository as a result of ingress of groundwater containing fertilizers. Moreover, nitrates may be generated by radiolysis of N_2. To complicate the problem further, species other than those currently identified as cracking agents also may promote cracking, because any species capable of promoting passivation also is a possible stress-corrosion cracking agent.

The results of the survey also indicated that the concentration of most of the species necessary to promote cracking was well above the values present in a typical basalt groundwater. However, most stress-corrosion cracking problems of technological importance occur in systems where the bulk environment is relatively innocuous, but where potent cracking environments develop locally, e.g., caustic cracking of boilers and carbonate/bicarbonate cracking of pipeline steels. Thus, one must examine the bulk environment to identify potential cracking agents and also examine possible mechanisms for increasing the concentrations of these agents.

A number of possible concentrating mechanisms for the cracking agents may operate in a waste repository. For example, during the thermal period but prior to pressure buildup, some boiling and resultant concentration may occur at or near the waste package. If localized corrosion occurs, anions will migrate into pits and crevices to maintain charge neutrality where hydrolysis occurs. Thermogalvanic corrosion can also promote concentration of species. Thermogalvanic corrosion, which can occur where there are gradients in the skin temperature of the overpack, separates the oxidation and reduction reactions, resulting in acidification at the anodic sites and hydroxide buildup at the cathodic sites.

This survey [2] also indicated that, in all of the systems for which electrochemical data are available, stress-corrosion cracking of carbon steel is associated with active/passive behavior and that the electrochemical potential range for stress-corrosion cracking is near to and more noble than the potentials at the peak current density, E_{max} (see Fig. 1). Moreover, it has been observed that severe cracking occurs in environments where i_{max}, as measured by the fast scan technique, is greater than about 1×10^{-3} A/cm^2 and where the peak current in the fast scan is at least an order of magnitude higher than the peak current in the slow scan.* Thus, electrochemistry is a useful tool for screening deleterious concentration ranges of known stress-corrosion cracking agents and in identifying potentially deleterious stress-corrosion cracking agents and synergistic interactions among species present in the basalt groundwater.

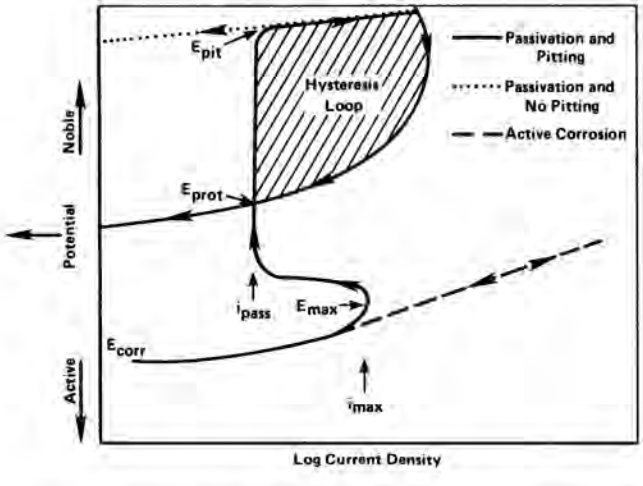

Fig. 1. Schematic of typical anodic potentiodynamic polarization curves.

E_{corr} = corrosion potential; E_{pit} = potential at which pits initiate on forward scan; E_{prot} = potential at which pits repassivate on reverse scan; i_{max} = current density at active peak; i_{pass} = current density in passive range.

It is also well-known that potentiodynamic polarization is a useful tool for studying pitting and crevice corrosion. Schematics of anodic polarization curves showing several types of behavior are given in Fig. 1. For the active corrosion case, the anodic curve is linear on an E-log i plot and the forward and reverse scans are coincident. The presence of a peak in the anodic portion of the curve is generally indicative of the onset of passivation. The occurrence of hysteresis between the forward and reverse scans is indicative of pitting. Where the hysteresis loop is very large, the protection potential may be very close to the open-circuit potential, indicating a high probability of pitting in service.

PROGRAM OBJECTIVE

The overall objective of the ongoing experimental program is to evaluate the influence of metallurgical and groundwater chemistry variables on the stress-corrosion cracking and pitting susceptibility of carbon steels in simulated basalt groundwater environments.

APPROACH

Potentiodynamic polarization curves were obtained on several carbon steels in simulated basalt groundwater environments and the potential susceptibility to stress-corrosion cracking and pitting were based on measurements of the appropriate electrochemical parameters. Initial experiments were performed on several steels in a standard simulated basalt groundwater composition to study the effect of metallurgical composition and structure on electrochemical behavior.

Subsequent studies of environmental effects were performed on a single hot rolled 1020 carbon steel composition. A list of environmental species was developed based on (i) the results of the literature survey in which known or suspected cracking agents were identified, (ii) analyses of typical basalt groundwater compositions and (iii) speculation concerning potential species that may intrude or be generated by radiolysis and thermal effects within the repository. A statistical experimental design of potentiodynamic polarization experiments was then used to determine the first and second order effects of each of these species on the electrochemical behavior.

EXPERIMENTAL PROCEDURES

Materials

The metallurgical studies were performed on three steel compositions, see TABLE I; (i)

* The potential scan rate used in generating a polarization curve can be varied. Fast scan curves generally refer to curves obtained at scan rates in excess of 10 V/h whereas slow scan curves refer to curves obtained at scan rates less than about 1 V/h.

TABLE I

Chemical Compositions, In Weight Percent, of Steels Used in the Experimental Program

Element	Proposed DOE Reference Steel	1020 Steel Specification Limits	Clean Carbon Steel	Doped Carbon Steel	Ferrovac E	Hot Rolled 1020 Carbon Steel
Carbon	0.15-0.20	0.18-0.23	0.18	0.17	0.003	0.2
Manganese	0.90 max	0.30-0.60	0.49	0.55	Tr[a]	0.46
Phosphorus	0.04 max	0.040 max	0.004	0.029	-	0.011
Sulfur	0.045 max	0.050 max	0.002	0.036	-	0.032
Silicon	0.60 max	-	0.30	0.35	Tr	0.17
Aluminum	-	-	0.10	0.14	Nil[b]	-
Copper	-	-	0.006	0.007	-	0.038
Nickel	-	-	0.002	0.004	Nil	0.014
Chromium	-	-	0.007	0.011	Nil	0.018
Molybdenum	-	-	0.000	0.000	Tr	0.024
Vanadium	-	-	0.000	0.006	-	-

(a) Tr = trace quantity detected

(b) Nil = none detected

"clean" carbon steel which has a composition similar to that of 1020 carbon steel, but with low phosphorus and sulfur, (ii) "doped" carbon steel which represents more typical commercial cleanliness, and (iii) Ferrovac E which is a low carbon, high purity steel. Both carbon steels were prepared from a split heat of a clean steel melt; the doped steel was produced by doping the clean melt with measured quantities of phosphorus and sulfur. As shown in TABLE I both steels meet a reference DOE steel specification but the clean steel has much lower sulfur and phosphorus concentrations.

The environmental studies were performed on a commercial hot rolled 1020 carbon steel having a composition shown in TABLE I.

All solutions were prepared with reagent grade chemicals and deionized water. The metallurgical studies were performed in a reference simulated basalt groundwater composition[3] which had a nominal composition of Na^+ - 360 wppm, K^+ - 3.4 wppm, Mg^+ - 0.03 wppm, Ca^{+2} - 2.8 wppm, F^- - 33 wppm, Cl^- - 310 wppm, SO_4^{-2} - 175 wppm, SiO_2 - 76 wppm, Total inorganic carbon 9 x 10^{-4} m/l, pH 25 C - 9.8. The environmental studies were performed on a 10X concentration of the above groundwater and on a series of solutions; the compositions of which are discussed in the results section.

The crushed basalt rock used in the experimental program was obtained from an outcropping of the umtanum flow and was prepared according to a standardized approach. The rock was initially crushed in a 3 inch jawcrusher, the weathered surfaces were removed, and the rock was recrushed in a 1 inch jawcrusher. The crushed rock was then graded in a rowtap shaker and -4+8 sieve material was stored for use in the experiments. Prior to testing, the crushed basalt rock was ultrasonically cleaned in distilled water and dried at 70 C for 4 hours.

Experimental Methods

Cylindrical specimens of dimensions 5.7 mm in diameter x 19 mm were machined from 6.35 mm diameter rod stock. Each specimen was then axially drilled and tapped (3-48). Specimen surfaces were prepared by abrading through No. 600 SiC and degreasing in acetone. A standard calomel reference electrode (SCE) and platinum counter electrode were used for the tests.

The experiments were carried out in a custom designed three-compartment glass cell. The working electrode cell is a double wall design and heat transfer fluid is circulated between the inner and outer walls to maintain the desired temperature during the testing.

The experiments were performed with a PAR Model 173 potentiostat, an ECO Model 567 function generator and a data acquisition system consisting of a Cyborg Model 91A-D converter and an Apple II computer.

Prior to testing, the electrochemical cell containing the electrolyte and the specimen was deaerated overnight by purging with argon or the desired gas mixture. Following deaeration, the polarization curve was obtained at the desired scan rate, either 0.6 V/hr (slow) or 18 V/hr (fast), starting 100 mV more negative than the free-corrosion potential. The scan was then reversed at a current density of approximately 2 x 10^{-3} A/cm^2 and terminated when the current on the reverse scan changed polarity. Values of E_{pit}, E_{prot}, E_{cor}, E_{max}, i_{max} and i_{pass} were extracted from the polarization curves, where applicable, as shown in Fig. 1. Values of i_{cor} were estimated by extrapolating the Tafel regions of the anodic and cathodic curves back to the corrosion potential.

Statistical Methodology

To be able to estimate the main effects of each of the environmental species of interest on the electrochemical behavior, a statistical design was used to define the optimal compositions of the test solutions. The statistical design was a partial factorial design of resolution IV. This design permits the main-effect terms of the

fifteen variables to be estimated free and clear of other main-effect terms and of any two-factor interactions. Three-factor and greater interactions still confound the main-effect terms; however, these usually contribute only a small response compared to the main-effect-term response. Consequently, a good estimate of the main-effect terms could be calculated at the end of the screening matrix of experiments.

Fifteen environmental species were selected for the study. These species fit into one or more of the following categories: (i) present in typical basalt groundwater, (ii) known stress-corrosion cracking agent for carbon steel, (iii) suspected stress-corrosion cracking agent for carbon steel, (iv) possible radiolysis product, and (v) suspected intrusion agent in repository. For the statistical design, high and low concentrations were selected for each of these species, see TABLE II. The low concentrations represent typical or nominal concentrations whereas the high concentrations were selected to demonstrate an effect. These high values are not necessarily intended to be realistic of in-service conditions. The statistical design gave 32 test solutions which were combinations of the high and low concentrations of species given in TABLE II. In addition, four experiments were performed using a midpoint for each species concentration to provide an estimate of error for the polarization experiments.

At the completion of the screening matrix of experiments, a regression analysis was performed on the different corrosion parameters with the aid of a multiple regression routine on the MINITAB statistical computer program. [4] The regression analysis calculated the "F" ratio and the regression coefficient for each of the fifteen species. The "F" statistic is a ratio of two variances, i.e., the sum of squares explained by each factor when entered in the equation, divided by the residual mean square (error). In general, when the calculated "F" ratio for a factor is large, it means that a large amount of experimental variation is explained by this term compared to the error variation. If a calculated "F" ratio exceeds the appropriate tabulated "F" value, then it can be assumed that the solution variable has a statistically significant effect on a particular polarization parameter. A 90-percent probability that a species is significant is usually acceptable for most experimental work and implies that one accepts a 10-percent chance of being incorrect in assuming that the factor has a significant effect.

TABLE II

High and Low Concentrations of Species Selected for Evaluation in the Electrochemical Experiments

	Species	High Concentration	Low Concentration
1.	pH	9.3	6.0
2.	Cl^{-1}	100,000 ppm	100 ppm
3.	F^{-1}	10,000 ppm	10 ppm
4.	Fe^{+2}/Fe^{+3}	Saturation	0.05 ppm
5.	Al^{+3}	1,000 ppm	0.1 ppm
6.	CO_3^{-2}/HCO_3^{-1}	1M	0.001 M
7.	NO_3^{-1}/NO_2^{-1}	1,000 ppm [N]	0.1 ppm [N]
8.	PO_4^{-3}	1,000 ppm [P]	0.1 ppm [P]
9.	$BO_3^{-3}/B_4O_7^{-2}$	1,000 ppm [B]	1 ppm [B]
10.	SiO_3^{-2}	1,000 ppm [Si]	10 ppm [Si]
11.	H_2O_2	100 ppm	0
12.	ClO_4^{-1}	100 ppm	0
13.	O_2	2% (Vapor)	0
14.	CO	1% (Vapor)	0
15.	H_2	80% (Vapor)	1%

The regression coefficients are multiplicative terms for the factors in a regression equation and were determined by a linear least square fit of the data. The regression coefficients determined in this study are calculated based on the high and low concentrations (+1 and -1) of the various chemical species. These factors are based on the design concentration range of the species. Because precipitation occurred in several solutions, the actual concentrations achieved in the test solutions were not the designed values. Therefore, the regression coefficients provide relative magnitudes of the measured effects only and are not meant to give a quantitative values of the effects. Solutions are in the process of being analyzed and actual chemical concentrations of the species examined will be used in the final analysis to provide the quantitative measure for the regression coefficients.

RESULTS

Metallurgical Effects

In the metallurgical effects studies, polarization experiments were performed in deaerated, simulated basalt groundwater at 90 C and a potential scan rate of 0.6 V/hr. The tests were performed on five steels: cast clean carbon steel, wrought clean carbon steel, cast doped carbon steel, wrought doped carbon steel, and Ferrovac E.

All of the steels exhibited similar behavior. A typical polarization curve is given in Fig. 2, where it can be seen that the steel exhibited active-passive behavior on the forward scan and

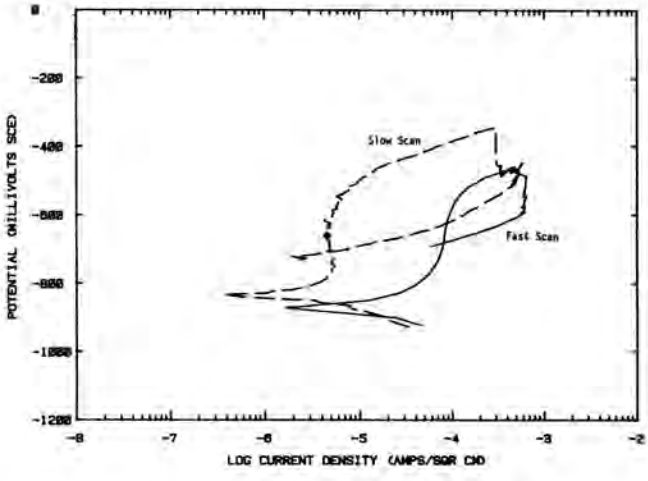

Fig. 2. Potentiodynamic polarization curves for cast carbon steel at two scan rates, fast (18 V/hr) and slow (0.6 V/hr) in deaerated basalt groundwater at 90 C.

hysteresis on the reverse scan. This hysteresis is indicative of pit initiation, which was confirmed by post-test examination of the specimen. A summary of the electrochemical results for all of the tests is given in TABLE III. These data show that neither the cleanliness of the steel or its structure (cast versus wrought) had a pronounced effect on its electrochemical behavior in the simulated basalt groundwater.

The active-passive behavior observed for these steels in basalt groundwater is similar to that reported for known stress-corrosion cracking agents for carbon steel, such as carbonate-bicarbonate. As discussed in the introduction, the fast scan - slow scan potentiodynamic polarization technique has been found to be useful in assessing the potency of an environment with regard to stress-corrosion cracking. Accordingly, this technique was applied to the carbon steel-basalt groundwater system. In the fast scan (18 V/hr) experiments, the curves were generated as soon as the specimen contacted the solution, whereas in the slow scan (0.6 V/hr), the specimens were allowed to equilibrate with the solution overnight as previously discussed. The aim of the fast scan polarization test was to obtain the maximum current density on relatively bare metal surfaces.

Figure 2, which contains a fast scan polarization curve for one steel, shows that passive currents were higher at the faster scan rate than at the lower scan rate; similar behavior was observed for the other steels. Empirically, it has been shown that stress-corrosion cracking susceptibility of carbon steel reaches a maximum at potential ranges where the differences in current density between these two curves are large. On this basis, one would expect that the most likely range for stress-corrosion cracking of carbon steel in basalt groundwater is between -0.78 V and -0.65 V (SCE). However, the differences between the fast and slow scan curves were small in comparison to differences observed in potent cracking systems. Thus, one would not expect a high degree of susceptibility to stress-corrosion cracking at 90 C in the nominal basalt groundwater composition.

Environmental Effects

Preliminary Experiments. Preliminary experiments were performed on two of the steels to evaluate the influence of groundwater concentration and leaching of basalt rock on the electrochemical behavior. For the leaching experiments, the groundwaters were equilibrated with crushed basalt rock by boiling overnight. In the concentration experiments, the concentrations of the species present in the basalt groundwater were increased 10-fold. These tests were performed to simulate conditions where boiling occurs adjacent to the overpack, resulting in groundwater concentration.

Results of these experiments are summarized in Figs. 3 and 4. These data show that there were small but systematic effects of groundwater concentration on the electrochemical behavior. The corrosion potentials (E_{cor}) and the potentials at the current peak (E_{max}) shifted to slightly more negative values and the passive current densities (i_{pass}) decreased slightly upon increasing solution concentration. On the other hand, no systematic effect of basalt rock leaching on the electrochemical behavior was evident.

Single and Combined Effects Studies. The results of the preliminary electrochemical experiments indicated that leaching of the basalt rock and uniform concentration of the groundwater did not have a pronounced effect on electrochemical behavior and, hence, on pitting and stress-corrosion cracking initiation. However, the concentration of one or several potent cracking or pitting species cannot be ruled out and, in fact, this behavior is commonly observed in systems in service. Accordingly, statistically designed experiments were initiated to evaluate the single and combined effects of species that may be present in the basalt repository and that may significantly influence the electrochemical behavior of carbon steel.

Potentiodynamic polarization curves were obtained on hot rolled 1020 carbon steel in 32 unique test solutions, which were combinations of high and low concentrations of the 15 solution variables, prepared according to the statistical design.

Figures 5 to 7 show polarization curves obtained in three of the 32 solutions; the compositions of these solutions are indicated in the figures. These polarization curves show the wide range of behavior observed by varying the concentration of the 15 species in the screening matrix of experiments. The polarization parameters selected from the curves also are shown in the figures. As can be seen, all of the polarization parameters cannot

TABLE III

Summary of Results of Potentiodynamic Polarization Tests Performed on Cast and Wrought Steels in Deaerated Basalt Groundwater at 90 C and a Scan Rate of 0.6 V/hr

Material	E_{cor}, V (SCE)	E_{max}, V (SCE)	E_{pit}, V (SCE)	E_{prot}, V (SCE)	i_{cor}, A/cm^2	i_{max}, A/cm^2	i_{pass}, A/cm^2
Cast Doped Carbon Steel	-0.840	-0.745	-0.508	-0.698	3.7×10^{-6}	5.5×10^{-6}	4.6×10^{-6}
Wrought Doped Carbon Steel	-0.859	-0.793	-0.481	-0.659	6.8×10^{-6}	1.2×10^{-5}	5.7×10^{-6}
Cast Clean Carbon Steel	-0.859	-0.793	-0.471	-0.679	6.2×10^{-6}	1.0×10^{-5}	6.2×10^{-6}
Wrought Clean Carbon Steel	-0.859	-0.801	-0.508	-0.669	3.4×10^{-6}	5.2×10^{-6}	4.4×10^{-6}
Cast Ferrovac E	-0.869	-0.764	-0.432	-0.679	6.2×10^{-6}	1.2×10^{-5}	6.2×10^{-6}

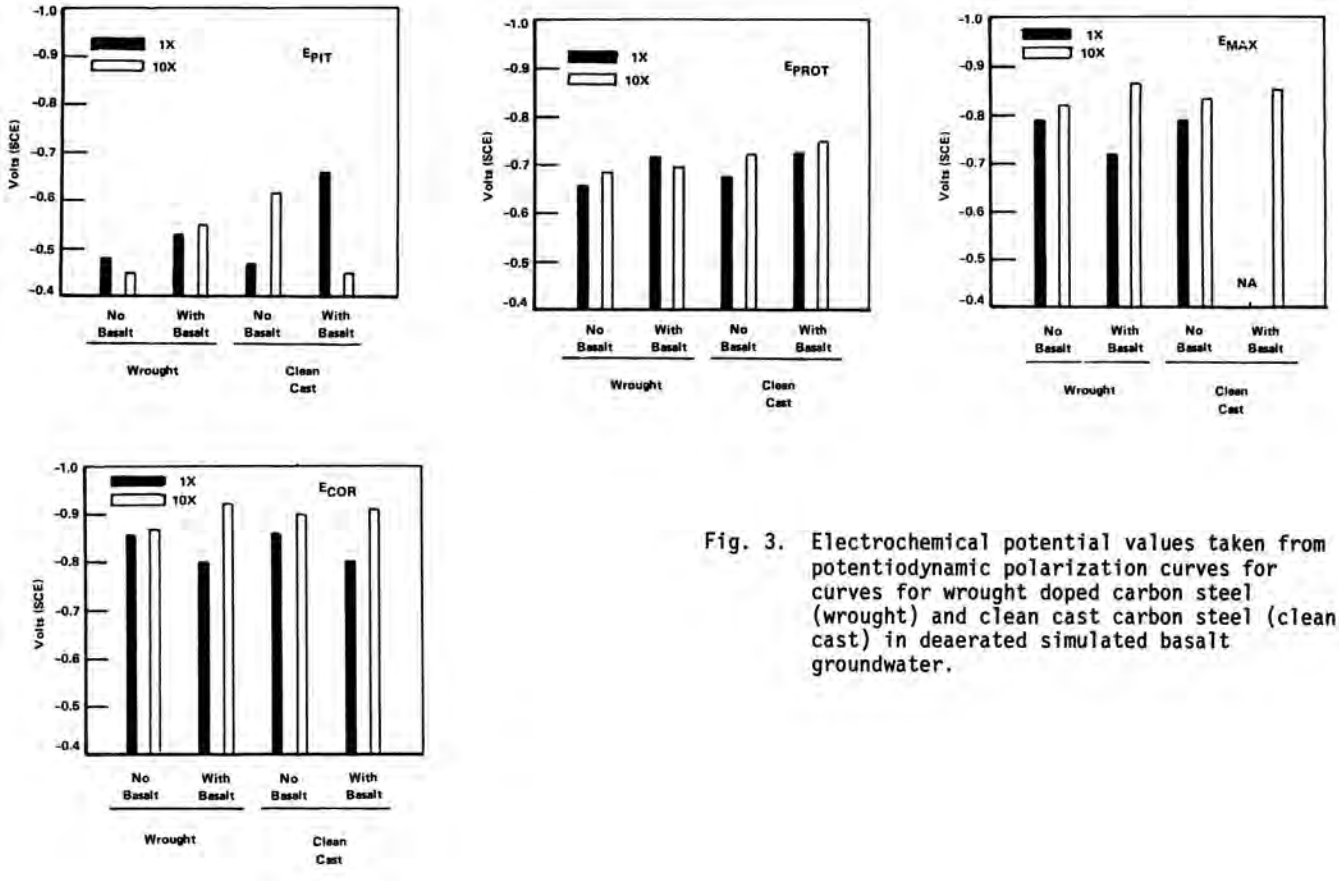

Fig. 3. Electrochemical potential values taken from potentiodynamic polarization curves for curves for wrought doped carbon steel (wrought) and clean cast carbon steel (clean cast) in deaerated simulated basalt groundwater.

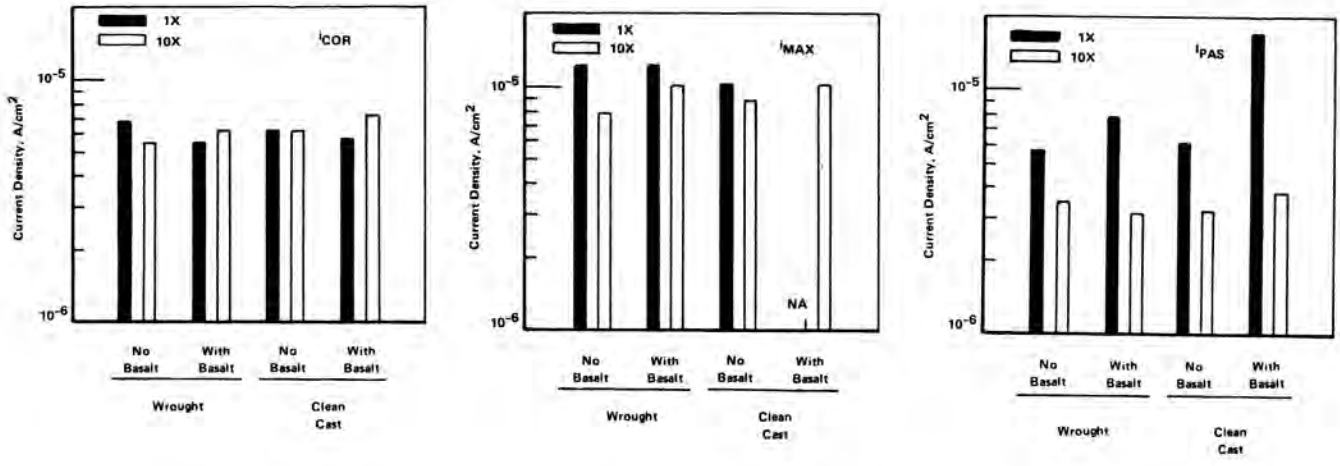

Fig. 4. Current density values taken from potentiodynamic polarization curves for wrought doped carbon steel (wrought) and clean cast carbon steel (clean cast) in deaerated simulated basalt groundwater at 90 C.

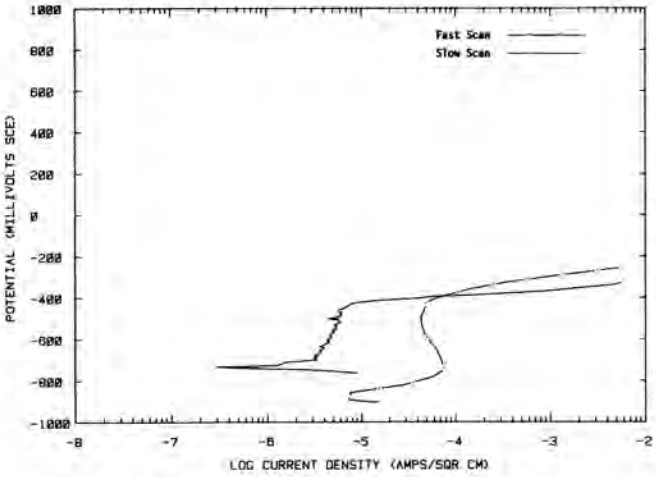

Fig. 5. Polarization curves for 1020 steel in solution 11, in which the following species were at the high concentration Cl, Fe, CO_3/HCO_3, BO_3/B_4O_7, H_2O_2, O_2, H_2.*

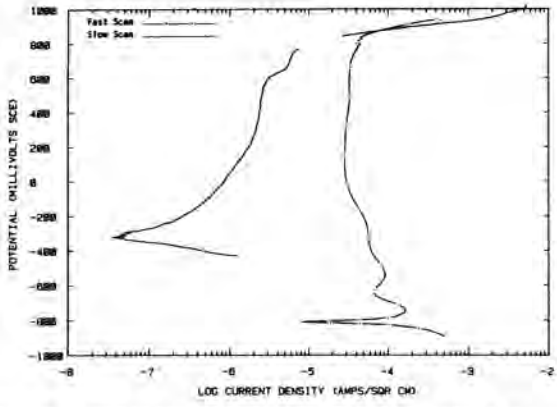

Fig. 6. Polarization curves for 1020 steel in solution 14, in which the following species were at the high concentration pH, F, Fe, CO_3/HCO_3, NO_3/NO_2, SiO_3, O_2.*

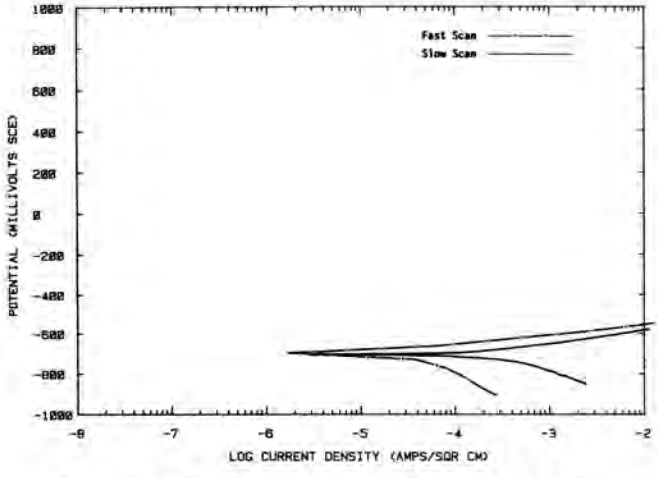

Fig. 7. Polarization curves for 1020 steel in solution 30, in which the following species were at the high concentration Cl, Al, PO_4, BO_3/B_4O_7, H_2O_2, ClO_4, CO, H_2.*

* The return scans were omitted for clarity.

be selected from each curve. For example, Fig. 7 shows no passive behavior and therefore i_{pas}, E_{pit}, and E_{prot} were not selected for this solution. TABLE IV shows the values for the polarization parameters for all 33 solutions that were used in the statistical analysis. The variations in the polarization parameters for the four tests repeated for solution 33 gives an indication of the reproducibility of the data obtained.

A statistical analysis was performed on each of the polarization parameters given in TABLE IV. The purpose of the analysis was to determine which of the 15 chemical species have a significant effect on the polarization behavior. TABLE V gives the results of the statistical analysis, indicating the main effect for each of the 15 species on the six polarization parameters examined. The "F" value indicates the significance of the species, and the coefficient indicates the relative magnitude of the effect. Coefficients are given

TABLE IV

Experimentally-Measured Polarization Parameters for the 33 Test Solutions

Solution	i_{cor} A/cm^2	E_{cor}, V(SCE)	i_{pas}, A/cm^2	E_{pit}, V(SCE)	E_{prot}, V(SCE)	$i_{max(fast)}$, A/cm^2
1	7.78 x 10^{-6}	-.422	2.21 x 10^{-5}	-.254	-.527	4.32 x 10^{-4}
2	2.0 x 10^{-7}	-.2	3.01 x 10^{-6}	.776	.776	2.23 x 10^{-5}
3	1.0 x 10^{-6}	-.574	4.61 x 10^{-6}	-.461	-.593	1.26 x 10^{-5}
4	7.32 x 10^{-7}	-.767	*	-.576	-.718	1.37 x 10^{-5}
5	1.0 x 10^{-4}	-.325	7.84 x 10^{-4}	1.0	1.0	1.87 x 10^{-3}
6	1.57 x 10^{-4}	-.859	8.97 x 10^{-5}	.808	-.808	2.46 x 10^{-3}
7	7.44 x 10^{-5}	-.515	9.33 x 10^{-4}	-.20	-.544	1.94 x 10^{-4}
8	4.21 x 10^{-5}	-.891	2.29 x 10^{-5}	-.042	-.625	1.57 x 10^{-3}
9	1.38 x 10^{-5}	-.781	1.30 x 10^{-5}	-.562	-.657	9.84 x 10^{-5}
10	1.1 x 10^{-6}	-.20	2.63 x 10^{-6}	.557	-.261	1.27 x 10^{-5}
11	2.97 x 10^{-6}	-.735	5.25 x 10^{-6}	-.422	-.64	7.49 x 10^{-5}
12	5.44 x 10^{-6}	-.623	2.73 x 10^{-5}	-.471	-.547	2.4 x 10^{-5}
13	5.74 x 10^{-5}	-.461	7.78 x 10^{-5}	-.33	-.471	7.5 x 10^{-4}
14	1.0 x 10^{-7}	-.31	2.42 x 10^{-6}	.808	.808	1.66 x 10^{-4}
15	8.51 x 10^{-5}	-.725	4.05 x 10^{-5}	-.557	-.64	1.37 x 10^{-4}
16	9.19 x 10^{-7}	-.515	2.73 x 10^{-6}	.54	-.452	1.32 x 10^{-4}
17	6.05 x 10^{-6}	-.657	1.11 x 10^{-5}	-.483	-.718	4.9 x 10^{-5}
18	8.97 x 10^{-6}	-.625	*	-.466	-.576	6.64 x 10^{-5}
19	5.83 x 10^{-6}	-.435	2.33 x 10^{-6}	.825	.776	5.24 x 10^{-5}
20	8.58 x 10^{-5}	-.498	1.32 x 10^{-4}	-.247	-.608	2.09 x 10^{-3}
21	2.03 x 10^{-6}	-.94	1.51 x 10^{-5}	.588	-.342	6.2 x 10^{-3}
22	5.08 x 10^{-5}	-.576	1.96 x 10^{-4}	-.42	-.515	5.30 x 10^{-5}
23	3.25 x 10^{-5}	-.876	6.53 x 10^{-5}	.745	.745	8.64 x 10^{-3}
24	2.12 x 10^{-6}	-.31	8.58 x 10^{-6}	.80	-.088	3.50 x 10^{-4}
25	6.0 x 10^{-6}	-.657	4.44 x 10^{-5}	-.40	-.576	2.73 x 10^{-5}
26	1.09 x 10^{-6}	-.64	*	-.483	-.718	1.49 x 10^{-4}
27	1.6 x 10^{-7}	-.562	7.38 x 10^{-7}	.083	-.53	4.08 x 10^{-5}
28	7.26 x 10^{-4}	-.688	*	*		3.33 x 10^{-3}
29	8.58 x 10^{-6}	-.562	1.07 x 10^{-4}	.80	-.042	2.71 x 10^{-3}
30	3.04 x 10^{-4}	-.703	*	*		*
31	6.43 x 10^{-4}	-.845	1.52 x 10^{-4}	.684	.684	3.37 x 10^{-3}
32	5.49 x 10^{-6}	-.781	6.25 x 10^{-6}	-.544	-.657	4.86 x 10^{-5}
33A	2.5 x 10^{-6}	-.544	6.25 x 10^{-6}	-.293	-.576	1.12 x 10^{-4}
33B	1.1 x 10^{-6}	-.466	3.73 x 10^{-6}	-.31	-.576	1.17 x 10^{-4}
33C	1.37 x 10^{-6}	-.53	4.27 x 10^{-6}	-.232	-.576	8.97 x 10^{-5}
33D	1.48 x 10^{-6}	-.53	4.61 x 10^{-6}	-.31	-.576	1.11 x 10^{-4}

*Not measured from polarization behavior.

only for those species that have a significant effect, based on a 75 percent or greater probability. For the majority of the discussions, a 90 percent or greater probability is typically required before an effect is considered significant. A positive coefficient indicates that an increase in concentration increases the value of the parameter, and a negative coefficient indicates that an increase in concentration of the species decreases the value of the parameter. TABLE V indicates that a majority of the species have an effect on at least one of the polarization parameters with the exceptions being perchlorate (ClO_4^-) and hydrogen (H_2), based on a 90 percent or greater probability of significance.

TABLE VI gives the results of the statistical analysis for the 15 groups of interactions that can be distinguished by the screening matrix design. The purpose of showing this table is to indicate that several of the two-factor interactions of the 15 species being examined are significant. Of particular interest to this program is the fact that several interactions are significant when considering i_{max}, which indicates the tendency for stress-corrosion cracking, and when considering E_{pit} and E_{prot}, which indicate the effects on pitting behavior.

TABLE VII summarizes the results of the statistical analysis for the main effects of the chemical species examined in the screening tests. Arrows are used to indicate the direction of the effect for each species that had a significant effect, based on a 90 percent or greater probability. Many of the effects were expected, such as O_2 and NO_3 increasing E_{cor} and CO_3^{-2}/HCO_3^- decreasing E_{cor}. Other effects, such as Cl^- decreasing E_{cor}, were not particularly expected but can be explained since Cl^- would tend to make the steel more active and would thereby decrease E_{cor}. It is also noteworthy that several species had a significant effect on i_{pas}. Referring back to TABLE V, NO_3^-/NO_2^- and $BO_3^{-3}/B_4O_7^{-2}$ had very large coefficients, indicating that these species greatly increased the passive current density with an increase in concentration, while SiO_3^{-2} and CO had large negative coefficients, indicating that these species greatly decreased i_{pas} with an increase in concentration.

The polarization parameter i_{max}, which is the maximum current density during the active peak, as measured with the fast scan technique, has been used to indicate the tendency for stress-corrosion cracking. Generally, a higher stress-corrosion cracking tendency is indicated by a larger i_{max}. As expected, CO_3^{-2}/HCO_3^- produced a significant increase in i_{max} with increasing concentrations. Chloride, on the other hand, decreased i_{max} with increasing concentration. This effect was not expected and will be considered more closely in the main matrix of experiments.

Pitting behavior also was affected significantly by some of the species. Chloride, as expected, tended to decrease E_{pit} and E_{prot}, indicating more severe pitting conditions. Oxygen, $BO_3^{-3}/B_4O_7^{-2}$ and pH all tended to increase E_{pit} and E_{prot} with increasing concentration.

As shown in TABLE VII, H_2 and ClO_4^- had no effect on the polarization parameters measured, based on a 90 percent or greater probability of significance. It should be noted, however, that ClO_4^- may have an effect that lasts for only a short period of time, and that it might have been overlooked in the present experiments. This issue will be addressed in follow-on studies.

DISCUSSION

Results of this study indicate that metallurgical structure, impurity level and minor variation in steel composition do not have a pronounced effect on the electrochemical behavior of the steels examined. Thus, one could conclude that the corrosion performance of a steel overpack could not be greatly improved by specifying a low impurity level such as is found in the clean steels, or by using a nearly pure iron, such as Ferrovac E. Several factors may temper this conclusion somewhat, however. First of all, little information is obtained from the potentiodynamic polarization technique on the propagation of pits, crevices, or cracks. Thus, alloy composition may not influence initiation greatly, but it is conceivable that propagation rates could be significantly affected. In addition, the potentiodynamic polarization technique is limited in that metallurgical effects on mechanical properties which in turn may influence stress-corrosion cracking susceptibility are not considered. Thus, it is well known that stress-corrosion cracking susceptibility of carbon steels decrease with decreasing carbon content, below about 0.1 percent carbon, even though this decrease is not evident in the electrochemical behavior. Finally, the influence of steel composition on the corrosion behavior of welds was not considered.

The results of the environmental studies clearly show that carbon steel exhibits active/passive behavior and hysteresis in simulated basalt groundwater. Thus, although rates of general corrosion may be lower than anticipated in this environment, pitting and crevice corrosion can occur and are the most probable failure modes. In addition, these electrochemical results, as well as the findings of the literature survey indicate that there is a possibility that stress-corrosion cracking of a carbon steel overpack will occur depending upon the concentration of species present.

The results of the environmental studies also indicated that the leaching of the basalt rock or a 10-fold increase in the basalt groundwater concentration did not have a pronounced effect on the electrochemical behavior. On the other hand, the results of the preliminary statistical matrix show that many of the species that are present in the groundwater or that may be generated or intrude in a repository potentially can have pronounced effects on the electrochemical behavior and hence on corrosion performance. With the completion of the statistical matrix of experiments and the subsequent analysis, these effects will be quantified and acceptable environmental ranges for performance will be estimated.

FOLLOW-ON STUDIES

Based on the results of the statistical analysis, 11 species were selected to be examined in a main matrix of experiments to quantify the main effects and two-factor interactions. TABLE VIII shows the 11 species that will be included in the main test matrix and the 21 two-factor interactions that will also be examined.

TABLE V

Results of Statistical Analysis Indicating the Effect of Each Chemical Species on the Polarization Parameters Measured by Potentiodynamic Polarization

	E_{cor}		$\log i_{cor}$		$\log i_{max}$		$\log i_{pas}$		E_{pit}		E_{prof}	
	F	Coef	F	Coef	F	Coef	F	Coef	F	Coef	F	Coef
pH	0.5		6.4	-0.34*	0.0		174	-0.18*	27	+0.31*	13	+0.22*
Cl	7.6	-0.06*	0.2		7.1	-0.23*	34	+0.06*	26	-0.25*	30	-0.32*
F	0.5		1.0		1.8	+0.11**	39	-0.08*	0.0		0.3	
Fe	0.9		0.9		0.2		86	+0.41*	0.0		0.3	
Al	1.1		0.8		0.0		36	+0.03*	1.7		0.1	
CO_3/HCO_3	8.4	-0.07*	0.3		25.1	+0.43*	3.6	-0.16**	2.9	+0.06**	0.9	
NO_3/NO_2	15.0	+0.09*	1.1		0.9		19	+0.64*	4.0	+0.13**	0.1	
PO_4	1.1		0.4		0.3		28	+0.10*	0.3		2.6	-0.10**
BO_3/B_4O_7	1.9	+0.03**	0.1		1.3		29	+0.78*	6.0	+0.14*	5.1	+0.13*
SiO_3	1.1		7.2	-0.36*	0.2		138	-0.85*	0.0		0.1	
H_2O_2	0.3		4.2	+0.27*	0.4		16	+0.25*	0.0		0.2	
ClO_4	0.2		0.1		0.0		1.2		0.2		1.3	
O_2	3.9	+0.05*	0.5		0.0		1.3		9.3	+0.13*	8.2	+0.15*
CO	0.1		0.1		0.0		22	-0.64*	1.1		0.0	
H_2	0.0		1.7	+0.17**	0.2		0.3		1.2		0.1	

*Greater than 90 percent probability that effect is significant.
**Greater than 75 percent but less than 90 percent probability that effect is significant.

TABLE VI

Results of Statistical Analysis Indicating the Effect of Groups of Interactions on the Polarization Parameters Measured by Potentiodynamic Polarization

	E_{cor}		$\log i_{cor}$		$\log i_{max}$		$\log i_{pas}$		E_{pit}		E_{prot}	
	F	Coef	F	Coef	F	Coef	F	Coef	F	Coef	F	Coef
ClxAl, $FxCO_3$, $FexNO_3$, $PO_4xH_2O_2$, BO_3xClO_4, SiO_3xO_2, $COxH_2$	1.3		0.6		2.9	-0.14**	61.2	-0.74*	0.0		0.7	
pHxAl, $FxPO_4$, $FexBO_3$, $CO_3xH_2O_2$, NO_3xClO_4, SiO_3xCO, O_2xH_2	3.3	-0.04**	0.3		0.0		144.8	-0.65*	0.1		0.4	
$pHxCO_3$, $ClxPO_4$, $FexSiO_3$, $AlxH_2O_2$, NO_3xO_2, BO_3XCO, ClO_4xH_2	2.1	-0.03**	6.5	+0.33*	24.2	+0.40*	852.6	+1.02	15.6	+0.20*	6.9	+0.15*
$pHxNO_3$, $ClxBO_3$, $FxSiO_3$, $AlxClO_4$, CO_2xO_2, PO_4xCO, $H_2O_2xH_2$	0.2		0.1		2.0	-0.12**	58.1	-0.08*	4.0	-0.13**	6.4	-0.12*
pHxCl, FxH_2O_2, $FexClO_4$, CO_3xPO_4, NO_3xBO_3, SiO_3xH_2, O_2xCO	0.4		0.3		4.8	+0.18*	47.3	-0.49*	2.2	-0.07**	9.1	-0.15*
pHxF, $ClxH_2O_2$, $FexO_2$, $AlxPO_4$, NO_3xSiO_3, BO_3xH_2, ClO_4xCO	0.1		2.3	-0.19**	8.5	-0.24*	53.7	+0.47*	0.8		0.6	
pHxFe, $ClxClO_4$, FxO_2, $AlxBO_3$, CO_3xSiO_3, PO_4xH_2, H_2O_2xCO	1.2		0.4		0.1		3.2	-0.01**	0.8		0.0	
ClxF, $pHxH_2O_2$, $FexCO$, $AlxCO_3$, NO_3xH_2, BO_3xSiO_3, ClO_4xO_2	0		0.1		0.8		136.7	+0.42*	0.7		0.4	
ClxFe, $pHxClO_4$, $FxCO$, $AlxNO_3$, CO_3xH_2, PO_4xSiO_3 $H_2O_2xO_2$	1.3		0.4		0.2		24.9	-0.09*	0.0		0.1	
$FxFe$, HxO_2, $ClxCO$, $AlxH_2$, CO_3xNO_3, PO_4xBO_3, $H_2O_2xClO_4$	2.0	+0.03**	0.4		2.7	-0.13**	11.2	-0.06*	0.6		0.2	
$FxAl$, $ClxCO_3$, $pHxPO_4$, $FexH_2$, NO_3xCO, BO_3xO_2, SiO_3xClO_4	5.0	-0.05*	9.9	-0.40*	0.7		7.9	+0.18*	10.5	+0.18*	0.7	
$FexAl$, $ClxNO_3$, $pHxBO_3$, FxH_2, CO_3xCO, PO_4xO_2, $SiO_3xH_2O_2$	0.1		0.6		0.6		--		0.1		0.5	
$FexCO_3$, $FxNO_3$, $pHxSiO_3$, $ClxH_2$, $AlxCO$, PO_4xClO_4, $BO_3xH_2O_2$	0.2		3.1	-0.23**	0.8		--		--		--	
$FexPO_4$, $FxBO_3$, $ClxSiO_3$, $pHxH_2$, $AlxO_2$, CO_3xClO_4, $NO_3xH_2O_2$	1.6		0.1		0.8		0.01		0.8		1.4	
$FexH_2O_2$, ClO_4xF, O_2xCl, $COxpH$, $AlxSiO_3$, CO_3xBO_3, NO_3xPO_4	0		0.5		0.0		--		0.2		2.3	-0.11**

*Greater than 90 percent probability that effect is significant.
**Greater than 75 percent but less than 90 percent probability that effect is significant.

TABLE VII

Summary of Results of Statistical Analysis for the Main Effects of the Chemical Species Based on a 90 Percent or Greater Probability of Significance

	E_{cor}	Log i_{cor}	Log i_{max}	Log i_{pas}	E_{pit}	E_{prot}
pH	-	+	-	+	+	+
Cl	+	-	+	+	+	+
F	-	-	-	+	-	-
Fe	-	-	-	+	-	-
Al	-	-	-	+	-	-
CO_3/HCO_3	+	-	+	-	-	-
NO_3/NO_2	+	-	-	+	-	-
PO_4	-	-	-	+	-	-
BO_3/B_4O_7	-	-	-	+	+	+
SiO_3	-	+	-	+	-	-
H_2O_2	-	+	-	+	-	-
ClO_4	-	-	-	-	-	-
O_2	+	-	-	-	+	+
CO	-	-	-	+	-	-
H_2	-	-	-	-	-	-

+ means that an increase in the control parameter, e.g., pH, resulted in an increase in the response parameter. - means that an increase in the control parameter resulted in a decrease in the response parameter.

TABLE VIII

Species and Interactions Selected from Screening Tests to be Examined in Main Test Matrix

Main Effects	Two-Factor Interactions	
pH	pH x Cl	Cl x H_2O_2
Cl	pH x CO_3	CO_3 x H_2O_2
F	pH x NO_3	CO_3 x O_2
Fe	pH x BO_3	NO_3 x BO_3
CO_3/HCO_3	pH x SiO_3	NO_3 x O_2
NO_3/NO_2	pH x H_2O_2	NO_3 x SiO_3
BO_3/B_4O_7	pH x O_2	BO_3 x SiO_3
SiO_3	pH x CO	BO_3 x H_2O_2
H_2O_2	Cl x CO_3	SiO_2 x O_2
O_2	Cl x NO_3	H_2O_2 x O_2
CO	Cl x BO_3	

REFERENCES

1. Title 10 Code of the Federal Regulations, Part 60, Federal Register, June 30, 1983.

2. Beavers, J. A., Thompson, N. G., and Parkins, R. N., "Stress Corrosion Cracking of Low Strength Carbon Steels in Candidate High Level Waste Repositories - Environmental Effects", Accepted for publication in Nuclear and Chemical Waste Management, December, 1984.

3. Jones, T. E., "Reference Material Chemistry - Synthetic Groundwater Composition", RHO, BW-ST-37P, April, 1982.

4. Minitab Project, Statistics Department, 215 Pond Laboratory, The Pennsylvania State University, University Park, PA, 16802, 1981.